A Study of Thin Film Resistor with High Resistivity.

Ying-Chieh Lee

Institute of Materials Engineering, National Pingtung University of Science and Technology
Tel : +886 8 7703202 ext 7556 / E-mail : YCLee@mail.npust.edu.tw

1. Introduction

Rapid technological advancements in many electronics industries, such as in the telecommunication and information, the aerospace, and the precision measurement sectors of industry, require the continuous development of electronic components to achieve higher precision, reliability, and integration [1]. Among these components, the resistor is one of the fundamental components and is primarily used in electronic circuits. In this respect, the demands for thin film resistors with low temperature coefficients of resistance (TCR) and high precision have been increasing dramatically in recent years [2–5].

2. Design Concept

The temperature coefficient of resistance (TCR) is an important technical parameter of thin film resistors. A high TCR will result in resistance value drifting and will consequently influence the accuracy of resistors as the temperature changes [6]. The main factors influencing the TCR include the sputtering process, annealing temperature, and film composition, whereas film composition plays a decisive role among these three factors. Therefore, employing an appropriate method for depositing a suitable film composition is the key to obtaining high-resistance resistors with a low TCR.

Extensive and rapid development in high entropy alloy has been conducted since the recent years by Yeh et al. [7]. These alloys are defined to have five or more principal metallic elements, with the concentration of each element varying between 5% and 35%. It is generally found that high entropy alloys form simple solid solution structures (rather than many complex phases) at elevated temperatures because of large mixing entropies. The simple crystal structures possess many excellent properties [8], such as easy of nanoprecipitation, high hardness, and superior resistance to temper softening, wear, oxidation, and corrosion.

3. Technical Development

Ni-Cr-Si-Al-Ta thin films of 80 nm in thickness were deposited on the substrates using a DC magnetron co-sputtering system having a sputtering rate of 5 nm/min. $Ni_{0.35}$-$Cr_{0.25}$-$Si_{0.2}$-$Al_{0.2}$ and tantalum of diameter 76.2 mm were used as targets. The sputtering chamber was evacuated to a background pressure of 7×10^{-7} Torr by a cryopump, and then the sputtering gas Ar with a purity of 99.999% at flow of 60 sccm was introduced into the chamber using mass flow controllers, by which the working pressure was 4.3×10^{-3}Torr. Thin films deposited on glass plates at room temperature were subjected to electron probe microanalysis (EPMA) and X-ray diffraction (XRD) studies, while thin films on Al_2O_3 substrates were used for measuring the electrical properties. The DC power was adjusted at 100 W and 200 W, respectively. The as-deposited films were annealed at 250 to 500℃ for 4 hours, with a heating rate of 5℃/min in air.

The sheet resistance R_s of the films was measured using the four-point probe technique, and the thickness t of the films was measured by FE-SEM (cross-section). The resistivity measured by the four-probe method was consistent with the resistivity obtained by the product of R_s and t. The TCR values of the Ni-Cr-Si-Al-Ta films were measured on thin long strips cleaved from the substrate. Electrical contacts to the two ends of the resistive strips were obtained by selectively coating the ends with sputtered Ag. The DC resistance of the strips was measured on digit multi meter (HP 34401A) at different temperatures (25℃and 125℃).

The composition of the deposited films was determined by Auger electron spectroscopy (AES). AES depth profiles were obtained in a PHI 550ESCA/SAM Auger microprobe (Physical Electronics, USA). The crystallinity of the films was analyzed by X-ray diffraction (XRD, Bruker D8A Germany),using Cu Kα radiation for 2θ values from 20°to 70°,with a scan speed of 3°min−1 and a grazing angle of 0.5°at 40 kV and 40 mA. Microstructural and thickness observations of the cross-sectional and plane-view morphology of thin films grown on glass substrates were analyzed by field-emission scanning electron microscopy (FE-SEM, Hitachi S-4700 Japan) with an accelerating voltage of 20 kV. The microstructure of the films was also investigated by a field-emission transmission electron microscope (FE-TEM, FEIE.O. Tecnai F20) equipped with an energy-dispersive spectrometer at an acceleration voltage of 200 kV. TEM specimens were prepared by disk cutting, mechanical polishing, dimpling, and ion milling.

4. Technological Competitiveness

Ni-Cr thin films are employed in integrated circuits, where low noise, good power dissipation, and a near-zero temperature coefficient of resistance are important requirements. Several studies have reported on the deposition of Ni-Cr resistive films by thermal evaporation [13–16] and radio frequency (RF) sputtering, primarily for use as hybrid resistors [17, 18]. Extensive work has been reported on the control of the sheet resistance Rs and TCR of Ni-Cr resistors by doping the films with different impurities. If silicon is added to the alloys, Ni-Cr-Si thin film resistors with very low temperature coefficients of resistivity are obtained, but the alloy resistivities are not significantly increased [1]. In our previous study, the effects of aluminum addition and annealing on the microstructure and electrical properties of Ni-Cr-Si films have been reported [19]. The electrical resistivities of the Ni-Cr-Si-Al films were higher than those of the Ni-Cr-Si films annealed at temperatures below 400°C, and the annealed Ni-Cr-Si-Al films exhibited a TCR close to zero. However, aluminum element has lower melting point (660°C), which is not good for stability. The tantalum, with high melting point is at 3020°C, will be being beneficial for thermal stability of resistive thin films [20].

To obtain resistive thin films with high resistivity and a low TCR, the concept of high entropy alloy was introduced to investigate the Ni-Cr-Si-Al-Ta composition as thin film resistors based on previously study of Ni-Cr-Si-Al thin resistor [19]. The effects of sputtering power and annealing temperature on the phases and microstructural and electrical properties of Ni-Cr-Si-Al-Ta thin films were investigated.

5. R&D Result

Electron probe microanalysis (EPMA) was used to determine the film compositions. The relative concentrations of nickel, chromium, silicon, aluminum, and tantalum were measured at three points in the sputtered films, respectively. The average values are listed in Figure 1. The results indicate that the composition of the sputtered Ni-Cr-Si-Al-Ta films with different sputtering powers were 23.5% Ni, 14.6% Cr, 23.6% Si, 16.8% Al, and 21.5% Ta at 100W and 24.5% Ni, 13.8% Cr, 23.6% Si, 17.6% Al, and 20.5%Ta at 200W, respectively. It was found that the Ta content was about 20%. However, these films are accorded to the rule of high entropy alloys which have five or more principal metallic elements with the concentration of each element varying between 5% and 35%.

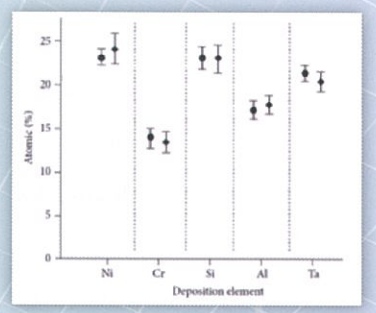

Figure 1: Compositions of Ni-Cr-Si-Al-Ta thin films with different DC sputtering powers sputtered on cooper sheet.

Figure 2 shows X-ray diffraction patterns of Ni-Cr-Si-Al-Ta films at 200W, for the as-deposited samples and those annealed at various temperatures for 240 min. All of the Ni-Cr-Si-Al-Ta films annealed at ≤400℃ exhibited an amorphous structure, indicating that none of the elements crystallized or oxidized. The term amorphous is a general term that refers to a solid state with a nonperiodical atomic arrangement. The characterization of an amorphous structure is much more difficult due to the broadening of diffraction patterns and the lack of reflections during X-ray investigations. Further study is needed to use transmission electron microscopy for crystalline analysis. It is interesting to point out that the Ni-Cr-Si-Al-Ta films did not oxidize after 500℃ annealing in air; there are only alloy phases formed in the Ni-Cr-Si-Al-Ta films. Yeh et al. [7, 22] reported that the HEAs can enhance the high temperature strength, corrosion, oxidation resistance, and so on.

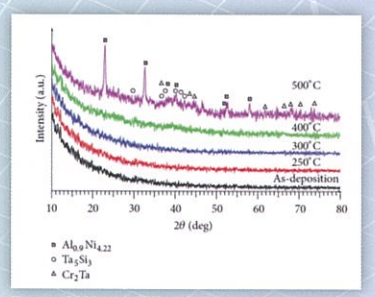

Figure 2: X-ray diffraction patterns of Ni-Cr-Si-Al-Ta thin films sputtered at 200W with different annealing temperatures.

Figure 3 shows X-ray diffraction patterns of Ni-Cr-Si-Al-Ta films with different sputtering powers on glass substrates, for as-deposited samples and those annealed at 500℃ for 240min. The figure shows that the as-deposited films had an amorphous structure. When the annealing temperature was set to 500℃, the crystallization of $Al_{0.9}Ni_{4.22}$, Ta_5Si_3, and Cr_2Ta was clearly discernible. In Figure 3 (b), which also shows the results at different sputtering power, the intensity of XRD peaks clearly increases with increasing sputtering power up to 200W. It indicates that the crystalline film is strongly influenced by the sputtering power when the films annealed at high temperature. This may be attributed to the fact that, at high sputtering power, the ejected metal atoms possess higher kinetic energy when they arrive on the substrate [23]. Consequently, these Ni, Cr, Si, Al, and Ta atoms have sufficient kinetic energy to rearrange themselves to form closer packing layer, resulting in a highly nanocrystalline film structure.

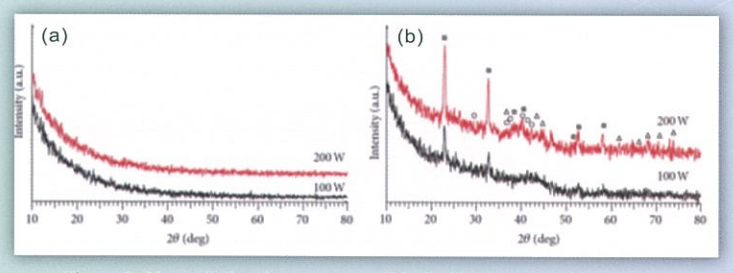

Figure 3: X-ray diffraction patterns of Ni-Cr-Si-Al-Ta thin films with different sputtering powers: (a) as-deposited and (b) annealed at 500℃

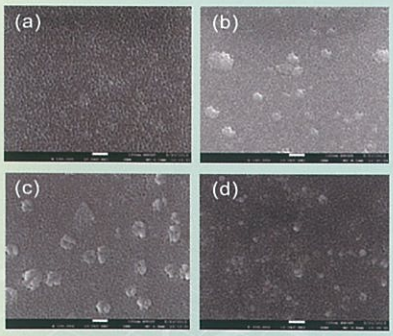

Figure 4: SEM micrographs of Ni-Cr-Si-Al-Ta films sputtered and annealed at
(a)200W/300℃ (b)200W/400℃
(c)200W/500℃ (d)100W/500℃

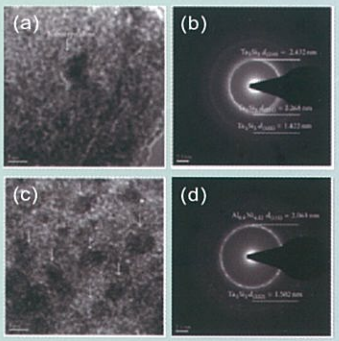

Figure 5: TEM micrographs and selected-area electron diffraction of Ni-Cr-Si-Al-Ta films sputtered and annealed at 200 W/300℃ for (a) and (b) and 200W/500℃ for (c) and (d).

Figure 4 shows SEM micrographs of the Ni-Cr-Si-Al-Ta thin films with different sputtering powers and annealing temperatures. Some heterogeneous phases appeared after annealing at 400℃ in the Ni-Cr-Si-Al-Ta thin films deposited at 200W, as shown in Figure 4(b), and it obviously appear after annealing at 500℃ as shown in Figure 4(c), which is consistent with the XRD analysis (Figure 2). These crystal phases should belong to $Al_{0.9}Ni_{4.22}$, Ta_5Si_3, and Cr_2Ta. For the Ni-Cr-Si-Al-Ta thin films deposited at 100W and annealed at 500℃, the heterogeneous phases were also observed, as shown in Figure 4(d).

Figure 5 shows a typical TEM bright field image and selected-area electron diffraction (SAED) patterns of the Ni-Cr-Si-Al-Ta thin films with different sputtering powers and annealing temperatures. For Ni-Cr-Si-Al-Ta thin films deposited at 200W and annealed at 300℃, it shows that the film with nanocrystalline structure appeared as shown in Figure 5(a). This result can be confirmed using the SAED patterns as shown in Figure 5(b). Therefore, the increase of sputtering power obviously causes the formation of a crystalline phase. With the annealing temperature increasing, more nanocrystallites were observed significantly to nucleate homogeneously throughout thin films and the SAED patterns changed to Debye-Scherrer-type rings (Figures 5(c) and 5(d)). However, the crystallites of the films annealed at 500℃ were obviously larger than the films annealed at 300℃. The phase analysis performed from the electron diffraction patterns enables the identification of $Al_{0.9}Ni_{4.22}$ and Cr_2Ta phases. The increase in peak intensities indicates an enhancement in the crystallinity of films because it is generally noted that the crystallinity can be enhanced while increasing the annealing temperature [27, 28].

Figure 6 shows the effect of annealing temperature and sputtering power on the electrical properties of the Ni-Cr-Si-Al-Ta films. The resistivity of Ni-Cr-Si-Al-Ta films decreases obviously with increasing of annealing temperatures. This result indicates that atomic configuration changes have occurred in Ni-Cr-Si-Al-Ta films. It is interesting to point that the resistivities of the Ni-Cr-Si-Al-Ta films are different between 100 and 200Wof sputtering power at 300℃ annealing. The resistivity of Ni-Cr-Si-Al-Ta films is ~2200 and ~1600 $\mu\Omega$-cm for 100W and 200W, respectively. There is more than 35% difference in resistivity between them. The reason for this is due to different crystal structures of Ni-Cr-Si-Al-Ta films with different sputtering power at 300℃; one is an amorphous at 100W and the other one is nanocrystalline at 200W. It is also interesting to note that the resistivity of the Ni-Cr-Si-Al-Ta films decreases with increasing the annealing temperature. From the above XRD and TEM results, the crystallinity of Ni-Cr-Si-Al-Ta films was enhanced with increasing the annealing temperature. In general, by increasing the annealing temperature, the resistivity of Ni-Cr-Si-Al-Ta films increases since the grain boundaries, crystal defects, and oxides generation of the film were increased [6]. In this investigation, the resistivity was decreased which can be attributed to an increase in alloy phases ($Al_{0.9}Ni_{4.22}$, Ta_5Si_3 and Cr_2Ta) with increasing the annealing temperature, as shown in Figures 2 and 5.

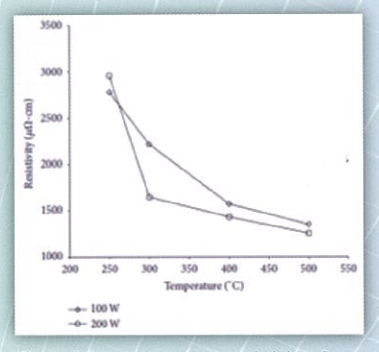

Figure 6: Room temperature resistivity of Ni-Cr-Si-Al-Ta films with different sputtering powers and annealing temperatures.

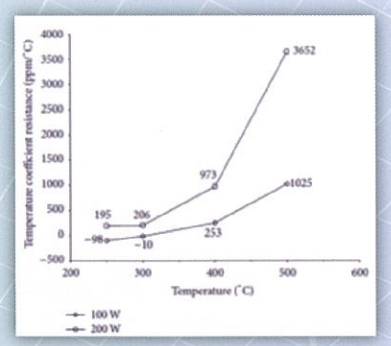

Figure 7: Temperature dependence of the TCR of Ni-Cr-Si-Al-Ta films with different sputtering powers and annealing temperatures.

Figure 7 shows the effect of annealing temperature and sputtering power on the temperature coefficient of resistivity (TCR) of the Ni-Cr-Si-Al-Ta films. The TCR values were increased with increasing of annealing temperature. TCR values were about 200 ppm/℃ annealed below 300℃ at 200W.Moreover, the Ni-Cr-Si-Al-Ta films deposited at 100W annealed at 300℃ exhibit a TCR close to zero because the films retain an amorphous structure after annealing. However, the TCR values of the films annealed at 500℃ are about 1000 ppm/℃. The TCR value becomes worse when the annealing temperature is increased. It can be explained that the annealing response of the TCR is the result of competition between a negative contribution from weak localization effects in the amorphous region and a positive contribution from crystalline phase grains [31]. For practical purposes, it is important for films with a small TCR to possess high resistivity.

References

1. Boong-Joo Lee, Duck-Chool Lee, Chul-Soo Kim, Electrical Properties of Sputtered Ni-Cr-Al-Cu Thin Film Resistors with Ni and Cr Contents, Journal of the Korean Physical Society, 40 [2] (2002) 339-343.
2. A. P. Bhatt, C. A. Luck and D. M. Stevenson, in Proc. Of the 1984 International symp. on microelectronics (1984), p. 370.
3. K. Matsuda, K. Sato, T. Doi, K. Ogata and K. Konishi, National Tech. Rep. 26, (1980), p. 283-288.
4. W. E. Isler and L. A. Kitchman, IEEE Trans. on Parts, Materials & Packaging PMP-5(3), 139 (1969).
5. E. Schippel, Kristall und Technik 15, 917 (1980).
6. X.Y. Wang, Z.S. Zhang, T. Bai, Materials and Design 31 (2010) 1302-1307.
7. Yeh J W, Chen S K, Lin S J, et al. Nanostructured High-entropy Alloys with Multi-Principal Elements-Novel Alloy Design Concepts and Outcomes. Advanced Engineering Materials, 2004, 6(5): 299-303.
8. Yeh J W, Chen S K, Gan J Y, et al. Formation of Simple Crystal Structures in Solid-Solution Alloys with Multi-principal Metallic Elements. Metallurgical and Materials Transactions A, 35A (2004) 2533-2536.
9. D.S. Campbell, B. Hendry, Br. J. Appl. Phys., 16 (1965) 1719-1722.
10. J.G. Swanson, D.S. Campbell, J.C. Anderson, Thin Solid Films 1 (1968) 325-342.
11. L. Lasak, L. Hieber, Thin Solid Films 17 (1973) 105-111.
12. G. Nocerine, K.E. Singer, Thin Solid Films 57 (1979) 343-348.
13. M. I. Birjega, C.A. Constantin, I.Th. Florescu, C. Sarbu, Thin Solid Films 92 (1982) 315-322.
14. S. Schiller, U. Heisig, K. Goedicke, H. Bilz, J. Henneberger, W. Brode, W. Dietrich, Thin Solid Films 119 (1984) 211-216.
15. S. Shiller, U. Heisig, K. Goedicke, H. Bilz, G. Pfeil, J. Henneberger, G. Vogler, Thin Solid Films 83 (1981) 165-172.
16. E. Schippel, Thin Solid Films 144 (1986) 21-28.
17. W. Gawalek, Thin Solid Films 116 (1986) 205-201.
18. J.H. Mooij, M. de Jong, J. Vac. Sci. Technol. 9 (1971) 446-449.
19. Seema Vinayak H.P. Vyas V.D. Vankar, Thin Solid Films 515 (2007) 7109-7116.
20. E. Schippel, Thin Solid Films, 146 (1987) 133-138.
21. Boong-Joo Lee and Duck-Chool Lee, Journal of the Korean Physical Society, 40 (2002) 339-343.
22. Dong-Jen Feng, Ying-Chieh Lee, Yi-Ben Chen, "A Study of Ni-Cr-Si-based Thin Film Resistors Prepared by DC Magnetron Sputtering" International Journal of Materials Engineering and Technology, 11 [2] (2014) 149-164.
23. S. Taioli, C. Cazorla, M. J. Gillan and D. Alfè, Melting curve of tantalum from first principles, PHYSICAL REVIEW B 75, 214103 (2007)
24. Chun Ng, Sheng Guo, Junhua Luan, Sanqiang Shi, C.T. Liu, Entropy-driven phase stability and slow diffusion kinetics in an Al0.5CoCrCuFeNi high entropy alloy, Intermetal lics 31 (2012) 165-172.
25. Ming-Hung Tsai and Jien-Wei Yeh, High-Entropy Alloys: A Critical Review, Mater. Res. Lett., 2 [3] (2014) 107–123.
26. André Anders, Joakim Andersson and Arutiun Ehiasarian, High power impulse magnetron sputtering: Current-voltage-time characteristics indicate the onset of sustained self-sputtering, Journal of Applied Physics, 102 (2007) 113303-1 - 113303-11.
27. D. J. Kwak, M. W. Park, and Y. M. Sung, Discharge power dependence of structural and electrical properties of Al-doped ZnO conducting film by magne tron sputtering (for PDP), Vacuum, 83 [1] (2008) 113–118.
28. Nirun Witit-Anun, Jakrapong Kaewkhao, Surasing Chaiyakun, Effect of Sputtering Power on Structural and Optical Properties of AlN Thin Film Deposited by Reactive DC Sputtering Technique, Advanced Materials Research, 770 (2013) 177-180.
29. Accarat Chaoumead, Youl-moon Sung, and Dong-Joo Kwak, The Effects of RF Sputtering Power and Gas Pressure on Structural and Electrical Properties of ITiO Thin Film, Advances in Condensed Matter Physics, 2012 (2012) 651587, 1-7.